ORIGINAL RESEARCH

Diffusion Tensor Imaging in Hydrocephalus: Initial Experience

Y. Assaf
L. Ben-Sira
S. Constantini
L.C. Chang
L. Beni-Adani

PURPOSE AND BACKGROUND: Diffusion tensor imaging (DTI) is an MR imaging–based technique that provides an in vivo tool for visualization of white matter tracts. In this preliminary study, we used this technique to investigate the diffusion characteristics of white matter tracts in patients with hydrocephalus before and after surgery and compared them with age-matched volunteers.

MATERIALS AND METHODS: Seven patients with different types of acute hydrocephalus (defined by acute clinical signs of increased intracranial pressure and imaging evidence of enlarged ventricles) underwent MR imaging including a DTI protocol before and after surgery for shunt placement/revision or ventriculostomy. Eight age-matched healthy subjects served as a control group. The DTI was acquired in a clinical setting that included 6 gradient directions with a b value of 1000 s/mm^2.

RESULTS: Before surgery, in fiber systems lateral to the ventricles (corona radiata), the diffusion parallel to the fibers was increased (+10%) and the diffusion perpendicular to the fibers was decreased (−25%) in all patients, resulting in an overall increase in the fractional diffusion anisotropy (FA, +28%). Following surgery, the FA values approached those of control values in all except 1 patient. In the corpus callosum, the presurgery FA values in patients with hydrocephalus (HCP) were lower than those of control values, and no significant changes were seen following surgery.

CONCLUSIONS: DTI can distinguish the compression characteristics of white matter before and after surgery in patients with HCP. At the acute stage of the disease, DTI characteristics point to white matter compression as a possible cause of the observed changes.

Increased intracranial pressure (ICP) is a major consequence of many intracranial pathologies, manifesting in headaches, vomiting, papilledema, and pupillary dilation due to herniation in extreme cases.[1,2] Increased ICP is frequently found in association with space-occupying lesions (tumors, hematomas, and abscesses), brain edema, and hydrocephalus (HCP),[1-5] conditions that can cause mechanical pressure and compression of brain tissue. To date, noninvasive imaging techniques such as MR imaging have been unable to evaluate ICP.[6] In HCP, conventional MR imaging sequences can demonstrate ventricular size and suggest areas of compressed tissue but cannot estimate local tension or pressure on the adjacent fibers.

The anatomic presence of ventriculomegaly by itself is not sufficient to diagnose HCP,[1,5] which by definition includes enlargement of ventricles with clinical symptoms and signs of elevated intracranial pressure. Differentiation of ventriculomegaly and the HCP syndrome can be difficult in patients with chronic conditions in whom enlarged ventricles have existed for a long time and/or clinical symptoms are subtle. Although HCP may require prompt surgical treatment, ventriculomegaly without elevated pressure may represent an old or compensated condition that should be followed conservatively.

Received December 2, 2005; accepted December 14.

From The Levie-Edersheim-Gitter Institute for Functional Brain Imaging (Y.A.), Tel Aviv Sourasky Medical Center and Tel Aviv University, Israel; the Department of Neurobiochemistry (Y.A.), Tel Aviv University, Tel Aviv, Tel Aviv, Israel; the Department of Neuroradiology (L.B.S.), Tel Aviv-Sourasky Medical Center, Tel Aviv, Israel; the Department of Pediatric Neurosurgery (S.C., L.B.A.), Dana Children's Hospital, Tel Aviv Sourasky Medical Center, Tel Aviv, Israel; the Sackler Faculty of Medicine (S.C.), Tel Aviv University, Tel Aviv, Israel; the Section on Tissue Biophysics and Biomimetics (L.C.C.), Laboratory of Integrative and Medical Biophysics, National Institute of Child Health and Human Development, The National Institutes of Health, Bethesda, Md.

Please address correspondence to Yaniv Assaf, MD, Department of Neurobiochemistry, Faculty of Life Sciences, Tel Aviv University, Tel Aviv, 69978, Israel; e-mail: asafyan@zahav.net.il

One can assume that increased ICP due to fluid accumulation in acute HCP leads to pressure on white matter pathways, especially those located around the ventricles.[3,7,8] Studies have shown that even chronic pressure to the white matter can lead to significant loss of neuronal transmission, demyelination, and axonal loss resulting in irreversible disability.[9-11] Diffusion tensor imaging (DTI) is an MR imaging–based technique that characterizes white matter.[12-16] DTI extracts the principal diffusivities (parallel and perpendicular to the fibers), the mean diffusivity (apparent diffusion coefficient [ADC]), and the fractional anisotropy (FA)—a measure of the difference between each of the principal diffusivities and the their mean.[13] The FA images provide very high contrast between gray and white matter: white matter appears hyperintense and gray matter, hypointense.

In contrast to the large number of studies on brain diseases with DTI, the technique has been used in only a few investigations of white matter compression (as happens in HCP).[17,18] Wieshmann et al showed that DTI can help delineate the displaced white matter and suggested that increased anisotropy might be related to white matter compression.[17,18] We undertook to evaluate whether changes in DTI indices before and after surgery can be used as a marker of white matter compression in HCP. To the best of our knowledge, this is the first study of the diffusion characteristics of pressed/tensed white matter tracts in HCP before and after surgery.

Methods

Patients. Seven patients with acute HCP and 8 age-matched healthy volunteers with no history of neurologic diseases, the control group, underwent MR imaging including DTI protocol. The patients with HCP underwent MR imaging before and after surgical intervention. Postsurgery MR imaging was performed at least 3 months following surgery to allow for re-adjustment of the tissue and intracranial pressure. Although MR imaging was performed as part of the

Patient details and clinical information

Patient No./ Age(y)/Sex	Basic Pathology	Presurgery Clinical Signs	Type of Surgery	Postsurgery Clinical Signs
1/12/F	Asymmetrical obstructive HCP	Headaches, vomiting, papilledema	Endoscopic septum pellucidotomy	Improved
2/13/M	Dandy walker variant, status after ventricular shunt	Headaches, vomiting, sleepy	VPS proximal revision	Improved
3/13/F	Meningocele, after meningitis, aqueductal stenosis	Vomiting, tremor, no papilledema	Endoscopic 3rd ventriculostomy	Slightly improved
4/12/F	Post IVH	Sleepy, headache, papilledema	Insertion of left VPS	Improved
5/14/F	Aqueductal stenosis	Loss of consciousness, disturbance in coordination	Endoscopic 3rd ventriculostomy	Improved
6/18/M	Tectal lesion (thick tectum)	Trembling, large head (>97th%), episodes of loss of consciousness, memory problems	Endoscopic 3rd ventriculostomy	Improved
7/20/F	Aqueductal stenosis	Learning disabilities, headaches, episodes of loss of consciousness	Endoscopic 3rd ventriculostomy	Improved

Note:—HCP indicates hydrocephalus; IVH, intraventricular hemorrhage; VPS, ventriculo-peritoneal shunt.

clinical assessments, the local institutional review board committee approved the MR imaging protocol, and informed consent was obtained from all participants or their parents/guardian. The patients' clinical and neurologic information is summarized in the Table.

Imaging Acquisition. MR imaging was performed on a 1.5T or 3T Signa scanner (GE Healthcare, Milwaukee, Wis) with a conventional quadrature head coil. The field of view in all MR imaging scans was 24 cm, and the section thickness was 3 mm with no gap between sections. In addition to several clinical sequences, the MR imaging protocol also included a T2-weight series (fast spin-echo pulse sequence with TR/TE, 5000/102 ms) and a DTI protocol. The DTI dataset was acquired by using a spin-echo diffusion-weighted echo-planar imaging sequence with the following parameters: TR/TE, 10000/98 ms; Δ/δ, 31/25 ms and g_{max} of 2.2 gauss/cm (for the 1.5T scanner); Δ/δ, 24/18 ms and g_{max} of 3.4 gauss/cm (for the 3T scanner); matrix dimension of 128 × 128, with 3 averages. The diffusion images were acquired along 6 noncollinear diffusion gradient directions with a maximal b value of 1000 s/mm^2. The DTI dataset consisted of 7 images (6 diffusion-weighted images and 1 with no applied diffusion gradients). The total acquisition time for the entire DTI dataset was 4 minutes.

Data Analysis. Before the diffusion tensor computation, all images were corrected for eddy current distortion and rigid-body brain motion by using the approach of Rohde et al.[19] Images were corrected by using a mutual information-based registration technique including a spatial transformation model for correcting eddy current–induced image distortion and head movements.[19] DTI analysis was performed as described by Basser and Pierpaoli.[12] Following image registration, 4 DTI-based images were used for region of interest (ROI)–based analysis: FA, ADC, $\lambda_\perp$ (radial diffusivity, perpendicular to the fibers, represented by the smallest eigenvalue), and $\lambda_{//}$ (parallel diffusivity, along the fibers, represented by the largest eigenvalue) images. ROIs were selected anatomically at the posterior limb of the internal capsule, the optic radiation, the superior longitudinal fascicules, the genu and splenium of the corpus callosum, the subcortical frontal white matter, and the subcortical temporal white matter. For each fiber system, ROIs were selected in at least 3 sections in which these fiber systems could be identified for each of the hemispheres. Because no statistical differences were found between left and right hemisphere data, we combined the information from both; thus, for each subject, numeric values of the different indices (FA, ADC, $\lambda_\perp$, and $\lambda_{//}$) were obtained by averaging the data from the 6 ROIs (3 per hemisphere).

Figure 1 is an example of ROI selection in a control subject and an HCP subject. To help with region of interest placement, we used color-coded FA maps in which white matter structures can be identified more easily.[15] In those maps, fibers crossing from left to right are visualized in red; those crossing posteroanteriorly are visualized in green; and those crossing inferosuperiorly, in blue. This methodology enables identification of a significant amount of well-documented white matter fiber systems.[20] Despite the significant displacement of the fibers by enlarged ventricles in our patients with HCP, the previously mentioned structures could be identified. An example is shown in Fig 1*G, -H*, in which ROI selections are shown for the patient with the largest ventricles (patient 3 in the Table). Comparison between the ROI groups (acute HCP → healthy controls; presurgery [acute] HCP → postsurgery HCP) was done by using the Student *t* test.

Results

Acute HCP was generally characterized by increased FA in areas of compressed white matter. Figure 2 shows the axial view of the ADC and FA images of 2 patients with HCP (Fig 2*B*, *-C*, and-*E*, *-F*, respectively) and a control subject (Fig 2*A*, *-D*) at the level of the internal capsule. Arrows point to significantly increased FA areas in the patients with acute HCP (Fig 2*E*, *-F*). In contrast, the ADC maps showed no significant differences between patients with HCP and control subjects. In contrast to the findings in fibers lateral to the ventricles, the corpus callosum parts (the body, the genu, and the splenium) that lie above the ventricles exhibited slightly reduced values of FA in patients with acute HCP compared with the control subjects. These areas were also characterized by increased ADC. Figure 3 shows the midsagittal view of the brain demonstrating the corpus callosum for a control subject and 2 patients with acute HCP. There is a marked reduction in the anisotropy, especially in the area of the genu (enlarged in the color scale) in the patients with HCP. The splenium was barely visible in most patients with HCP and could not be analyzed. Except for the internal capsule and the genu of the corpus callosum, other ROIs (superior longitudinal fascicules, sub-

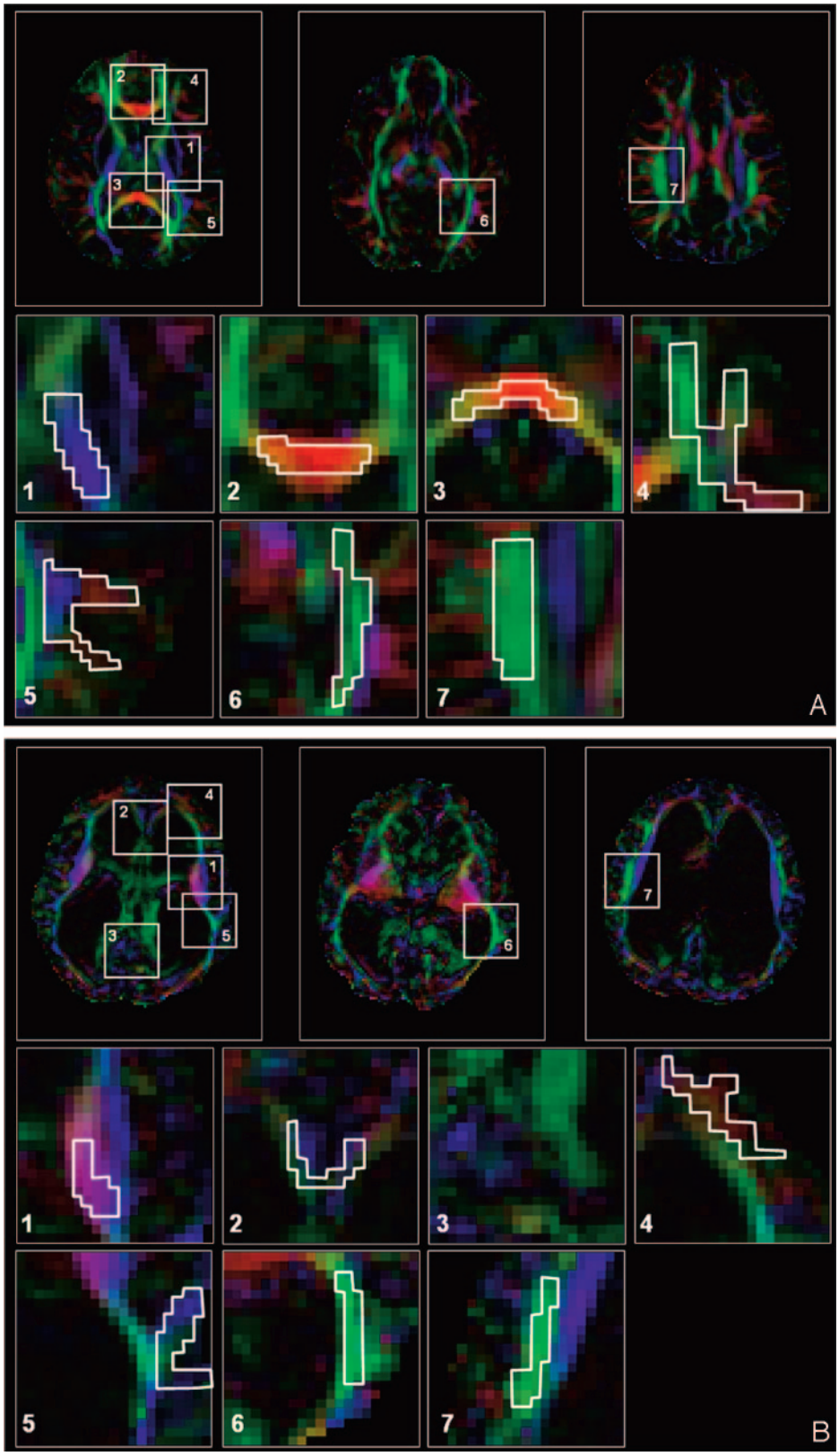

Fig 1. ROI selection in a control subject (*A*) and a patient with acute HCP (*B*). *A,* Three representative images of color-coded FA maps. Using a DTI-based atlas of white matter tracts, one can define specific white matter fascicules.[20] Superimposed polygons on color-coded maps identifies the 7 ROI groups that were analyzed in this study (magnified below). For each ROI group, data were measured in another 2 sections and for the left and right hemispheres (not shown). The ROI groups include the following: the posterior limb of the internal capsule,[1] the genu of the corpus callosum,[2] the splenium of the corpus callosum,[3] the subcortical frontal white matter,[4] the subcortical temporal white matter,[5] the optic radiation,[6] and the superior longitudinal fascicules.[7] *B,* The same ROI groups are used for the patient with acute HCP with the largest ventriculomegaly. All ROI groups except the splenium of the corpus callosum could be identified for this patient.

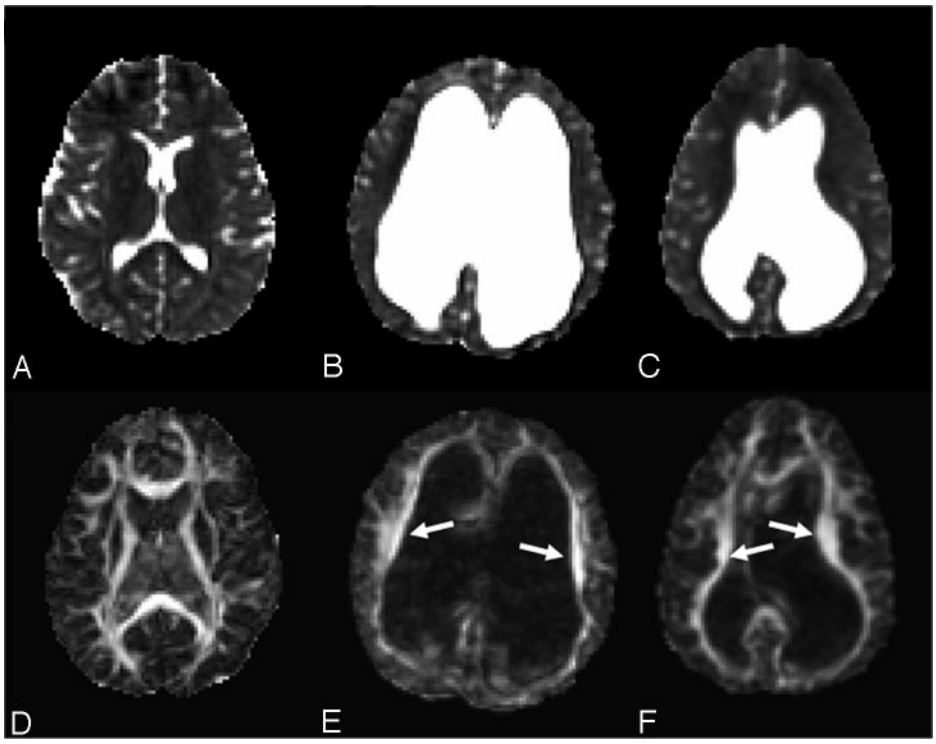

Fig 2. ADC (top row) and FA (bottom row) of a healthy subject (*A* and *D*), and 2 patients with acute HCP (*B* and *F*, patients 3 and 1 in the Table). The patients with HCP show significantly increased ventricular volume with significant asymmetry in one of them (*C*). FA maps of the 2 patients with acute HCP show increased FA in corona radiata fibers (*arrows*) and normal ADC values (*C* and *F*).

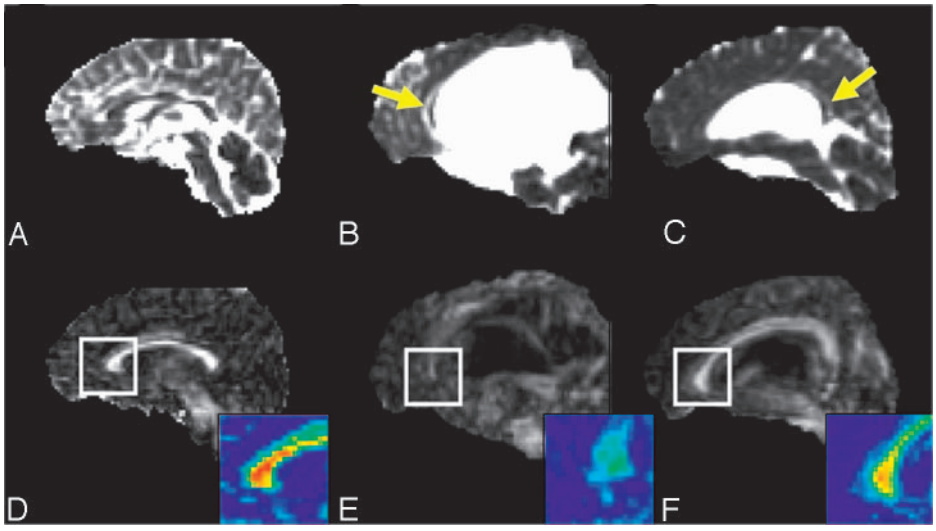

Fig 3. Midsagittal view of the 3 subjects shown in Fig 1 depicting the genu, splenium, and body of the corpus callosum. Top row: ADC images. Bottom row: FA maps. In the patients with HCP, the corpus callosum is displaced superiorly (*B–F*) and appears generally degenerated. The displaced corpus callosum has slightly elevated ADC (*yellow arrows*) and reduced FA (see enlarged color scale images) compared with those areas in control subjects (*A* and *B*).

cortical frontal white matter, subcortical temporal white matter, and optic radiation) showed less significant changes.

Figure 4 summarizes the ROI analysis for the internal capsule and the genu of the corpus callosum. In the internal capsule (Fig 4*A*, -*B*), the FA was 0.74 ± 0.11 for the group with acute HCP and 0.58 ± 0.03 for the control group. The ADC did not differ significantly between the 2 groups: 0.67 ± 0.01 and 0.70 ± 0.03 for the control and HCP groups, respectively. In the genu of the corpus callosum (Fig 4*C*, -*D*), the FA was 0.47 ± 0.08 for the acute HCP group and 0.72 ± 0.03 for the control group. In this region, the ADC was higher for the HCP group than for the control group: $0.98 \pm 0.13 \times 10^{-5}$ cm^2/sec versus $0.76 \pm 0.03 \times 10^{-5}$ cm^2/sec, respectively. Other regions (superior longitudinal fascicules, subcortical temporal white matter, subcortical frontal white matter, and optic radiation) followed the trend of the internal capsule, but differences were slight and not statistically significant.

Six of the 7 patients with HCP underwent MR imaging before and after shunt implantation or endoscopic surgery. All except 1 patient (patient 3, Table) showed improvement in clinical signs following surgery and significant changes in the diffusion parameters. A considerable reduction in the FA was observed in most analyzed regions (including the internal capsule, corona radiata, optic radiation, and superior longitudinal fascicules). Again, the most striking effect was in the internal capsule and corona radiata, but other areas exhibited a noticeable decline as well. Figure 5 shows ADC and FA maps of a patient with HCP before and after surgery. The 2 MR imaging scans were registered; therefore, the sections are at similar locations. The shrinkage in CSF volume following surgery is apparent in the ADC images. The reduction in FA is apparent in the internal capsule area (the left internal capsule is magnified in the color scale). Figure 5*E*, -*F* shows ADC and FA ROI analyses for the internal capsule: the FA decreased from 0.72 ±

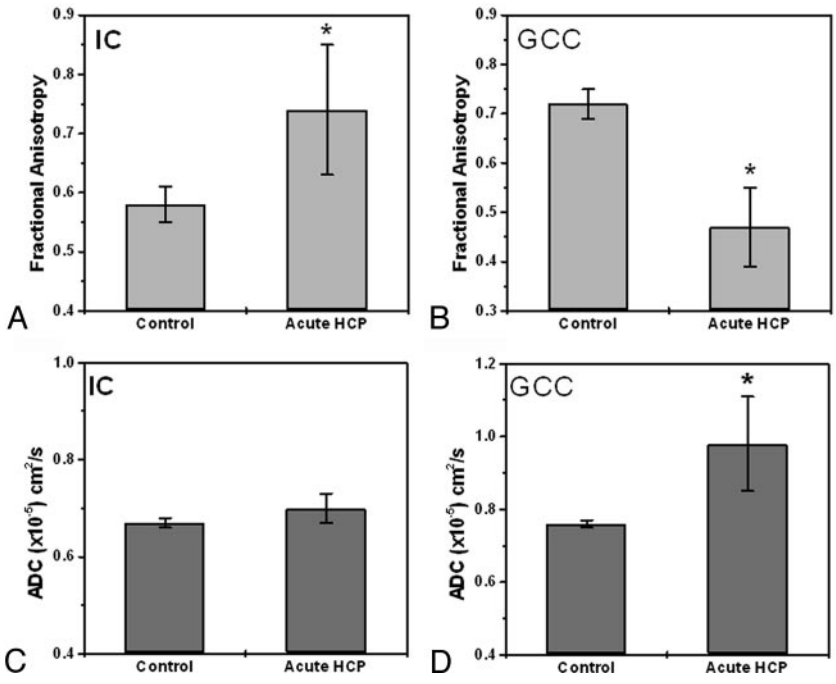

Fig 4. ROI analysis of FA and ADC values in the internal capsule and genu of the corpus callosum for controls and patients with acute HCP (data are the mean of all patients in each group). *A,* FA values in the internal capsule are significantly increased ($P < .001$) for the patients with acute HCP compared with control subjects. *B,* FA values in the genu of the corpus callosum are significantly decreased ($P < .01$) for the patients with acute HCP compared with control subjects. *C,* ADC values in the internal capsule are similar for all subjects with no statistical difference between the 2 groups. *D,* ADC values in the genu of the corpus callosum are significantly higher for the patients with acute HCP ($P < .01$) compared with the control subjects.

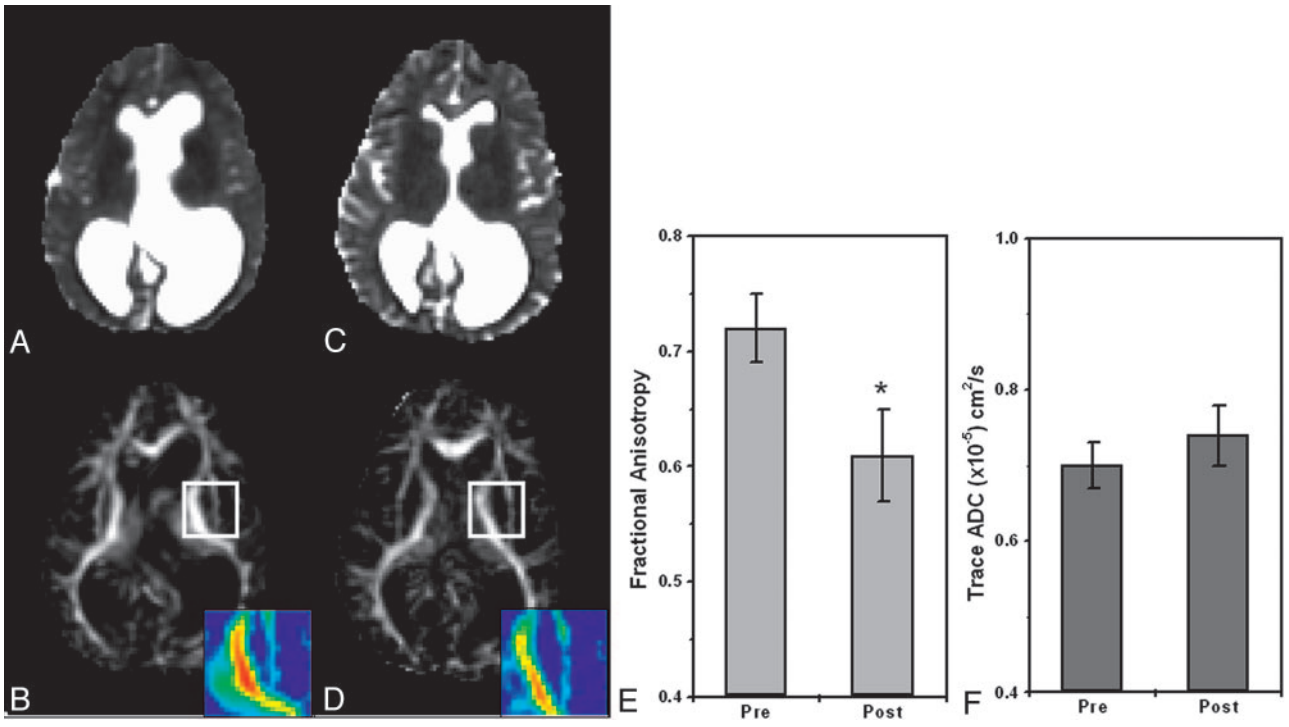

Fig 5. Pre- and postsurgery DTI-based images at similar section locations for patient 1 (Table). The patient underwent endoscopic septum pellucidotomy. ADC maps before (*A*) and after (*C*) surgery show significant reduction in ventricle volume with no apparent change in ADC values. FA maps before (*B*) and after (*D*) surgery show significant reduction in FA values of the internal capsule after surgery (see enlarged color-scale images). *E* and *F,* ROI analyses for the same patient before and after surgery: FA is significantly reduced after surgery ($P < .001$) in the internal capsule, whereas ADC values remain the same.

0.03 before surgery to 0.61 ± 0.04 after surgery, and the ADC remained nearly the same. For this patient, only the superior longitudinal fascicules showed a similar trend of FA reduction (from 0.55 ± 0.04 to 0.50 ± 0.06), whereas other regions stayed the same (the optic radiation, the splenium of the corpus callosum, the genu of the corpus callosum, the subcortical frontal white matter, and the subcortical temporal white matter) before and after surgery. Figure 6 shows this analysis for another patient. Like the previous patient, FA values decreased from 0.65 ± 0.03 before surgery to 0.52 ± 0.07 after surgery at the level of the internal capsule, whereas ADC values remained constant. Other regions showed no significant changes for this patient.

To learn more about the origin of the FA changes in acute HCP signs, we decomposed the FA into its diffusivities ($\lambda_\perp$ and $\lambda_{//}$) and analyzed each one separately. Areas of increased

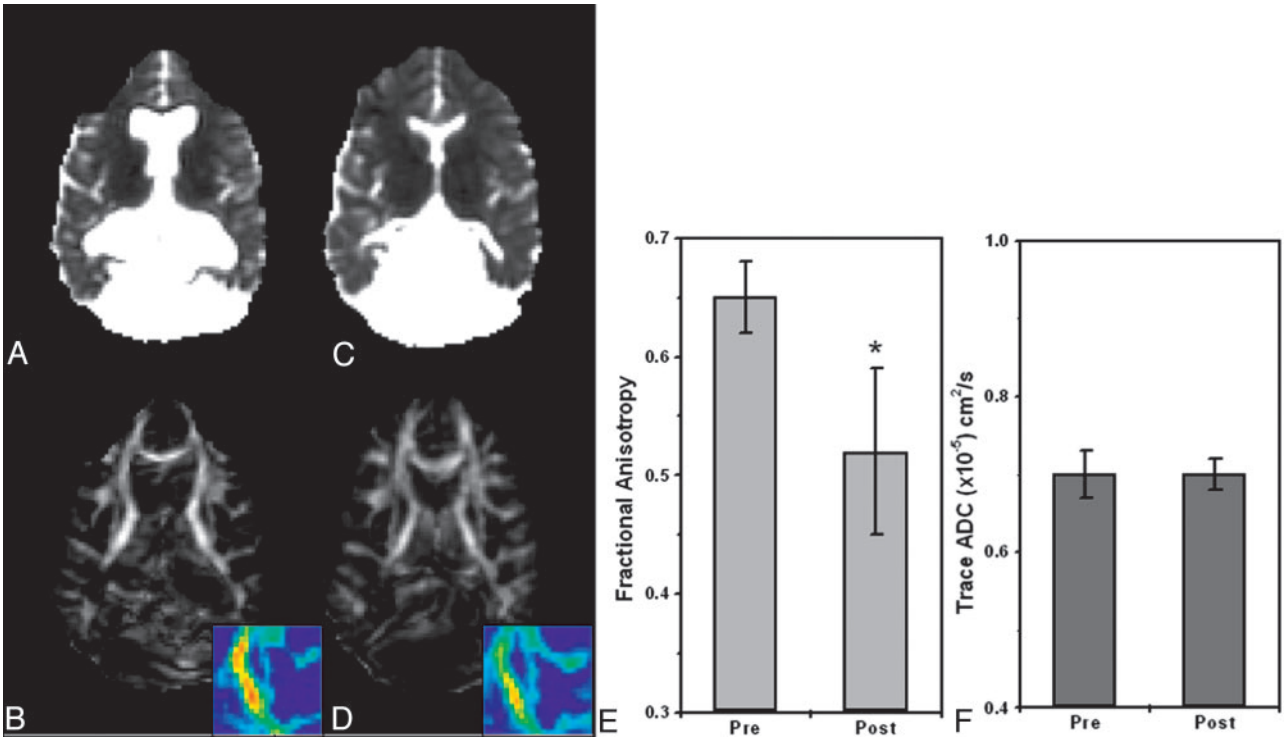

Fig 6. Pre- and postsurgery DTI-based images at similar section locations for patient 2 (Table). The patient underwent ventriculoperitoneal shunt proximal revision. ADC maps before (*A*) and after (*C*) surgery show significant reduction in ventricle volume with no apparent change in ADC values. FA maps before (*B*) and after (*D*) surgery show significant reduction in FA values of the internal capsule after surgery (see enlarged color-scale images). *E* and *F*, ROI analysis for this patient before and after surgery: FA is significantly reduced after surgery ($P <$ .001) in the internal capsule, whereas ADC values remain the same.

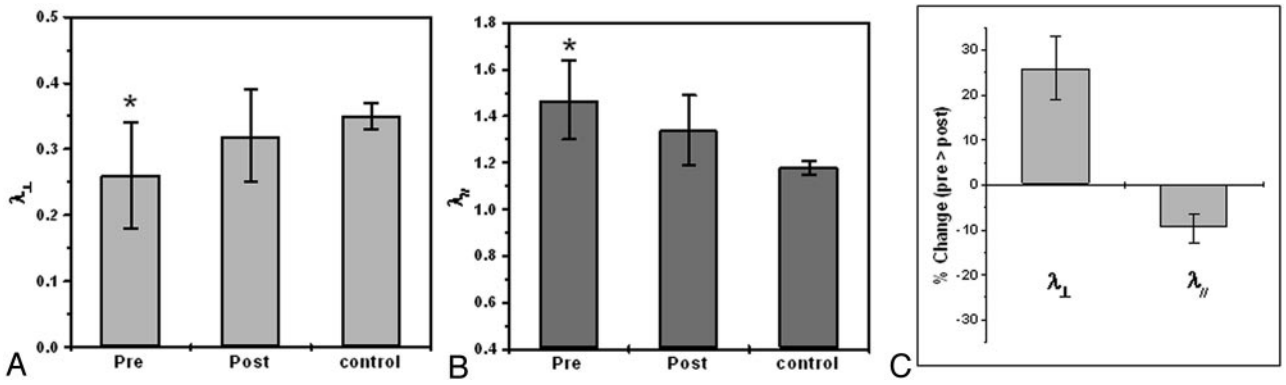

Fig 7. ROI analysis for patients with acute HCP, before and after surgery at the level of the internal capsule (data are averaged over all patients in each group). *A*, Analysis of the radial diffusivity shows significantly lower values before surgery compared with those of control subjects and increased values after surgery approximating control values. *B*, Analysis of the parallel diffusivity shows significantly higher values before surgery compared with those of control subjects and decreased values after surgery approximating control values. *C*, To reduce intersubject variability, we compared data for each subject with his or her own presurgery values; this analysis showed ~25% increase in radial diffusivity and ~10% decrease in parallel diffusivity after surgery.

anisotropy showed reduced diffusivity perpendicular to the fibers and increased diffusivity parallel to the fibers. This resulted in an increase in the overall FA and no net change in the ADC. Figure 7 graphically summarizes these observations. Figure 7*A* depicts the perpendicular diffusivity of patients with acute HCP and the control group before and after surgery averaged across all subjects and patients. A significant increase in perpendicular diffusivity to normal values was seen after surgery ($P < .05$, paired *t* test). The same analysis for the parallel diffusivity (Fig 7*B*) showed a significant reduction in the diffusivity after surgery, albeit not to control values. To overcome intersubject variability, expressed by the large error bars, we normalized each subject to the presurgery values (Fig 7*C*). This analysis revealed a highly significant increase of ~25% in the radial diffusivity after surgery, accompanied by a significant decrease of ~10% in the parallel diffusivity.

Discussion

The main finding of this study was that the FA was increased in the white matter areas lateral to the ventricles in acute HCP. The increased volume of the CSF in HCP frequently leads to pressure on the most adjacent white fiber pathways: the corona radiata and the corpus callosum.[21,22] In the corona radiata, we observed a significant increase in the FA (especially in the internal capsule), evidenced by an increase in the parallel diffusivity and a decrease in the radial diffusivity (Figs 2 and

4). The opposite trend was observed in the corpus callosum: reduced FA, reduced parallel diffusivity, and increased radial diffusivity (Figs 3 and 4). In fact, the corpus callosum in patients with HCP had diffusion characteristics similar to degenerated white matter tissue. Pre- and postsurgery examinations of the patients with HCP revealed significant improvement after surgery in the FA values (especially of the internal capsule), which approximated control values (Figs 5 and 6). Postsurgery DTI showed no changes in diffusion characteristics of the corpus callosum.

Increased Versus Decreased FA

Most DTI studies on neuronal diseases and disorders report reduced FA generally associated with neuronal degeneration, as in multiple sclerosis, or edema, as in stroke.[22-30] In those diseases, the FA reduction is accompanied by an increase in ADC and a dramatic elevation in the radial diffusivity values.[31-33] In patients with HCP, such diffusion characteristics are found in the corpus callosum, leading to the assumption that the corpus callosum undergoes neuronal degeneration. Studies on pathology of the corpus callosum in acute and chronic HCP support this observation.[34-36]

In contrast to FA reduction in the corpus callosum in acute HCP, the FA is increased in white matter lateral to the ventricles. A marked decrease in the radial diffusivity accompanied by an increase in the parallel diffusivity caused the ADC values to remain at control levels because ADC averages all diffusivities. Similar results were found on diffusivity analyses of displaced white matter by brain tumors.[37] From these observations, it can be assumed that direct pressure to the white matter affects the white matter architecture in a way that causes the FA to increase.

The different pattern of changes in the internal capsule and the genu of the corpus callosum might represent different pathophysiologic mechanisms. Because all our patients were clinically diagnosed with acute HCP, it is reasonable to assume that high ICP was present in all of them (although not monitored). If the previous assumptions about the mechanisms that cause the FA changes (ie, degeneration for reduced FA and displacement of increased FA) are true, one can speculate that the corpus callosum is the tissue most affected by the enlarged ventricles (because it is located just above them) and therefore degenerates more rapidly. The corona radiata, which lies lateral to the ventricles, might experience milder pressure than the corpus callosum and, therefore, appear as only displaced. Even in cases of chronic HCP (arrested HCP), other studies found that the white matter is also degenerated in the lateral fiber systems.

Possible Mechanism of Increased FA

A possible explanation for the observed increased FA in acute HCP is the morphologic changes that occur in fiber architecture under mechanical pressure (which probably happens in HCP). For homogeneously aligned white matter fibers, mechanical pressure will cause higher packing of the fibers and increased fiber density per unit area. Higher axonal density will increase the tortuosity of water molecules, which might lead to overall reduction in the measured radial diffusivity. This increased tortuosity should be a direct consequence of extracellular tissue shrinkage and is expected to happen in compression. Indeed, this is observed in stroke, in which cytotoxic edema leads to extracellular space shrinkage and overall slowed diffusivity.[23]

In contrast to the radial diffusivity, which is influenced by the geometric packing of the fibers, the parallel diffusivity is relatively free of obstacles. Nevertheless, we observed an increase in the parallel diffusivity under mechanical pressure. This might reflect stretching of the fibers to be more linearly aligned, resulting in fewer obstacles to diffusion and faster diffusion. Indeed, the effect parallel to the fibers was found to be smaller than that on the radial diffusivity (10% versus 25%).

Limits of the Application of DTI in Increased ICP

Increased ICP may also happen in cases in which no mechanical pressure is apparent (eg, pseudotumor cerebri). Assuming that the changes observed in acute HCP are a result of the changes to the microarchitecture of the fibers (ie, a secondary effect of the increased ventricles size), it is unlikely that such changes will be found in cases of increased ICP without massive tissue compression. Moreover, although increased FA was also found in space-occupying lesions, in which the adjacent tissue is obviously compressed by the lesion volume,[37] other white matter areas in the brain of such patients show normal FA and diffusivity, though they undergo significant pressure.

Thus, increased FA might be a unique characteristic of acute HCP and could serve as a diagnostic criterion, but one must take into account the patients with HCP in whom the enlarged ventricles represent a chronic condition of the brain. Such patients, often referred to as having "arrested HCP," show no clinical symptoms of increased ICP. The brain in these cases has most probably compensated for loss of space by increased tissue density (ie, more white matter fibers per unit area). Some of these patients may have a high FA as well. On the other hand, long exposure of the tissue to unnatural compression could result in tissue degeneration,[35] throwing into question whether DTI can characterize arrested HCP.

Future Work

This preliminary study raises questions about ICP and white matter. One question is the appearance of DTI in patients with arrested HCP: can DTI distinguish between arrested HCP and acute HCP? If so, DTI could become a powerful tool for radiologic assessment and management of HCP. Another question is whether our findings can be generalized to other ages. Our study included patients older than 9 years even though most patients with HCP are in early childhood. This age cohort was chosen for 3 reasons: 1) FA changes stemming from normal development are relatively minor after the age of 5–6 years,[38] so any changes in FA in an individual can be attributed only to the surgical intervention and not to other developmental factors. 2) The study of young patients with HCP is complicated by development-related FA changes, in addition to those caused by the enlarged ventricles. 3) The recruitment of an age-matched control group for young patients is difficult. Thus, future studies on the efficacy of using DTI in HCP will have to include a large number of patients and control subjects with a wide range of ages. Last, a study should be performed on both arrested and treated patients with HCP, in whom the diffusion parameters are evaluated for a long period of time (a

few years) in the same brain region. Such a study will contribute to the assessment of tissue degeneration in chronic (arrested) and short-term HCP.

Conclusions

The fact that DTI shows 2 patterns of changes (increased versus decreased FA) raises speculation about the micron-scale changes of the tissue and the pathophysiologic mechanisms it undergoes in HCP. The measurement and analysis of the principal diffusivities together with FA offer the possibility to follow and characterize pressure effects on white matter tracts in HCP. The demonstration that DTI can quantify changes before and after surgery might give the radiologist a tool with which to estimate tissue recovery, and it can give the neurosurgeon an indicator, in addition to clinical improvement, of the effectiveness of surgery, especially in patients in whom there is a decrease in ICP with no evident decrease in the size of the ventricles, as often happens after endoscopic surgeries.

Acknowledgments

This research was supported by the Israel Science Foundation, grant no. 1280/04.

References

1. Czosnyka M, Pickard JD. **Monitoring and interpretation of intracranial pressure.** *J Neurol Neurosurg Psychiatry* 2004;75:813–21
2. Williams MA, Razumovsky AY. **Cerebrospinal fluid circulation, cerebral edema, and intracranial pressure.** *Curr Opin Neuro.* 1993;6:847–53
3. Del Bigio MR. **Neuropathological changes caused by hydrocephalus.** *Acta Neuropathol* 1993;85:573–85
4. Del Bigio MR. **Pathophysiologic consequences of hydrocephalus.** *Neurosurg Clin N Am* 2001;12:639–49
5. Bradley WG Jr. **Diagnostic tools in hydrocephalus.** *Neurosurg Clin N Am* 2001; 12:661–84
6. Filley CM, ed. **The behavioral neurology of white matter.** New York: Oxford University Press; 2001
7. Del Bigio MR, da Silva MC, Drake JM, et al. **Acute and chronic cerebral white matter damage in neonatal hydrocephalus.** *Can J Neurol Sci* 1994;21:299–305
8. Fletcher JM, Bohan TP, Brandt ME, et al. **Cerebral white matter and cognition in hydrocephalic children.** *Arch Neurol* 1992;49:818–24
9. Bergstrom K, Thuomas KA, Ponten U, et al. **Magnetic resonance imaging of brain tissue displacement and brain water contents during progressive brain compression: an experimental study in dogs.** *Acta Radiol Suppl* 1986;369: 350–52
10. O'Brien JP, Mackinnon SE, MacLean AR, et al. **A model of chronic nerve compression in the rat.** *Ann Plast Surg* 1987;19:430–35
11. Siegal T, Siegal TZ, Sandbank U, et al. **Experimental neoplastic spinal cord compression: evoked potentials, edema, prostaglandins, and light and electron microscopy.** *Spine* 1987;12:440–48
12. Basser PJ, Pierpaoli C. **A simplified method to measure the diffusion tensor from seven MR images.** *Magn Reson Med* 1998;39:928–34
13. Pierpaoli C, Basser PJ. **Towards a quantitative assessment of diffusion anisotropy.** *Magn Reson Med* 1996;36:893–906
14. Pierpaoli C, Jezzard P, Basser PJ, et al. **Diffusion tensor MR imaging of the human brain.** *Radiology* 1996;201:637–48
15. Pajevic S, Pierpaoli C. **Color schemes to represent the orientation of anisotropic tissues from diffusion tensor data: application to white matter fiber tract mapping in the human brain.** *Magn Reson Med* 1999;42:526–40
16. Basser PJ, Mattiello J, LeBihan D. **MR diffusion tensor spectroscopy and imaging.** *Biophys J* 1994;66:259–67
17. Eriksson SH, Rugg-Gunn FJ, Symms MR, et al. **Diffusion tensor imaging in patients with epilepsy and malformations of cortical development.** *Brain* 2001;124(Pt 3):617–36
18. Wieshmann UC, Symms MR, Parker GJ, et al. **Diffusion tensor imaging demonstrates deviation of fibers in normal appearing white matter adjacent to a brain tumour.** *J Neurol Neurosurg Psychiatry* 2000;68:501–03
19. Rohde GK, Barnett AS, Basser PJ, et al. **Comprehensive approach for correction of motion and distortion in diffusion-weighted MRI.** *Magn Reson Med* 2004;51:103–14
20. Mori S, Wakana S, Nagae-Poetscher LM, et al. eds. *MRI Atlas of Human White Matter.* 1st ed. Amsterdam, The Netherlands: Elsevier Science: 2004
21. Del Bigio MR. **Cellular damage and prevention in childhood hydrocephalus.** *Brain Pathol* 2004;14:317–24
22. Sundgren PC, Dong Q, Gomez-Hassan D, et al. **Diffusion tensor imaging of the brain: review of clinical applications.** *Neuroradiology* 2004;46:339–50. Epub 2004 Apr 21
23. Sotak CH. **The role of diffusion tensor imaging in the evaluation of ischemic brain injury: a review.** *NMR Biomed* 2002;15:561–69
24. Lim KO, Helpern JA. **Neuropsychiatric applications of DTI: a review.** *NMR Biomed.* 2002;15:587–93
25. Le Bihan D, Mangin JF, Poupon C, et al. **Diffusion tensor imaging: concepts and applications.** *J Magn Reson Imaging* 2001;13:534–46
26. Graham JM, Papadakis N, Evans J, et al. **Diffusion tensor imaging for the assessment of upper motor neuron integrity in ALS.** *Neurology* 2004;63:2111–19
27. Thomalla G, Glauche V, Koch MA, et al. **Diffusion tensor imaging detects early Wallerian degeneration of the pyramidal tract after ischemic stroke.** *Neuroimage* 2004;22:1767–74
28. Pfefferbaum A, Sullivan EV. **Increased brain white matter diffusivity in normal adult aging: relationship to anisotropy and partial voluming.** *Magn Reson Med* 2003;49:953–61
29. Kealey SM, Kim Y, Provenzale JM. **Redefinition of multiple sclerosis plaque size using diffusion tensor MRI.** *AJR Am J Roentgenol* 2004;183:497–503
30. Iannucci G, Rovaris M, Giacomotti L, et al. **Correlation of multiple sclerosis measures derived from T2-weighted, T1-weighted, magnetization transfer, and diffusion tensor MR imaging.** *AJNR Am J Neuroradiol* 2001;22:1462–67
31. Song SK, Yoshino J, Le TO, et al. **Demyelination increases radial diffusivity in corpus callosum of mouse brain.** *Neuroimage* 2005;26:132–40
32. Thomalla G, Glauche V, Weiller C, et al. **Time course of wallerian degeneration after ischaemic stroke revealed by diffusion tensor imaging.** *J Neurol Neurosurg Psychiatry* 2005;76:159–60
33. Nair G, Tanahashi Y, Low HP, et al. **Myelination and long diffusion times alter diffusion-tensor-imaging contrast in myelin-deficient shiverer mice.** *Neuroimage* 2005;28:165–74
34. Ding Y, McAllister JP 2nd, Yao B, et al. **Axonal damage associated with enlargement of ventricles during hydrocephalus: a silver impregnation study.** *Neuro Res* 2001;23:581–87
35. Del Bigio MR, Wilson MJ, Enno T. **Chronic hydrocephalus in rats and humans: white matter loss and behavior changes.** *Ann Neurol* 2003;53:337–46
36. Del Bigio MR, Zhang YW. **Cell death, axonal damage, and cell birth in the immature rat brain following induction of hydrocephalus.** *Exp Neurol* 1998; 154:157–69
37. Assaf Y, Pianka P, Rotshtein P, et al. **Deviation of fiber tracts in the vicinity of brain lesions: evaluation by diffusion tensor imaging.** *Isr J Chemistry* 2003;43: 155–63
38. Schneider JF, Il'vasov KA, Hennig J, et al. **Fast quantitative diffusion-tensor imaging of cerebral white matter from the neonatal period to adolescence.** *Neuroradiology* 2004;46:258–66